Annals of Nuclear Medicine Vol. 19, No. 1, 29–33, 2005

Washout rates of Tc-99m tetrofosmin in asymmetric septal hypertrophy

Gülgün BÜYÜKDERELİ,* Mehmet KANADASI** and Mustafa KIBAR*

*Departments of *Nuclear Medicine and **Cardiology, Cukurova University Faculty of Medicine, Adana, Turkey*

The aim of this study was to evaluate the washout rate of Tc-99m tetrofosmin in asymmetric septal hypertrophy (ASH). As Tc-99m tetrofosmin accumulation and retention depend on sarcolemmal and/or mitochondrial function, the presence or absence of abnormalities in the washout rate of Tc-99m tetrofosmin could provide information about sarcolemmal and/or mitochondrial damage noninvasively. The study group consisted of 18 patients with ASH and 10 healthy subjects. After intravenous injection of 1,110 MBq (30 mCi) Tc-99m tetrofosmin, tomographic images were obtained 1 hour later (early image) and again 4 hours later (delayed image). Using tomographic images, the distribution and washout of tetrofosmin in the left ventricle was examined quantitatively. Short-axis SPECT images were divided into 5 segments (anterior, septal, lateral, inferior wall and apex) in early and delayed images, and the mean radioactivity counts were measured in each segment by drawing regions of interest. Washout rates of apex, anterior, septal, lateral and inferior walls were 0.34 ± 0.06, 0.37 ± 0.07, 0.36 ± 0.07, 0.33 ± 0.08, 0.33 ± 0.07 in ASH and 0.20 ± 0.05, 0.23 ± 0.05, 0.22 ± 0.03, 0.21 ± 0.03, 0.22 ± 0.03 in the normal group, respectively. In ASH, the washout rates of all myocardial segments were significantly increased as compared to those of the normal controls ($p < 0.05$). The findings of the present study suggest that there could be dysfunction of sarcolemma and/or mitochondria in the entire left ventricle which would be important in the pathophysiology of this disease. Also our study revealed that Tc-99m tetrofosmin washout was higher in NYHA II–III patients compared to NYHA I patients and the degree of Tc-99m tetrofosmin washout corresponded well with the thickness of the interventricular septum and posterior walls.

Key words: Tc-99m tetrofosmin, washout rate, asymmetric septal hypertrophy

INTRODUCTION

HYPERTROPHIC CARDIOMYOPATHY is an inherited disease defined as a heart muscle disorder of unknown origin.[1,2] Asymmetric septal hypertrophy (ASH) is the most frequent type of ventricular muscle hypertrophy.[3,4] Pathophysiology of this disease is unclear.[5,6] Disorganized arrangement of cardiac muscle cells has been recognized to be an important morphologic feature of the ventricular architecture in this disease.[7,8] Tc-99m tetrofosmin is a widely used myocardial perfusion agent with advantageous imaging characteristics. Once this tracer is taken up by the myocardium, its clearance is relatively slow, and redistribution does not occur for several hours.[9,10] Its accumulation and retention depend on cell membrane and/or mitochondrial potentials indicating cell viability and metabolically active cells.[11–13] Thus, Tc-99m tetrofosmin scintigraphy can be useful for evaluating sarcolemmal and/or mitochondrial function as well as perfusion abnormalities. The present study was performed to evaluate the washout rate of Tc-99m tetrofosmin in ASH. The presence or absence of abnormalities in the washout rate of Tc-99m tetrofosmin can provide information about sarcolemmal and/or mitochondrial damage noninvasively.

Received June 30, 2004, revision accepted October 18, 2004.

For reprint contact: Gülgün Büyükdereli, M.D., Kurtuluş mah. Ziyapaşa Bulvarı, Büşra apt. Apt No: 10 Daire No: 15, 01130 Seyhan, Adana, TURKEY.

E-mail: gulgunb@cu.edu.tr

MATERIALS AND METHODS

Subjects

The study group consisted of 18 patients with ASH (10 men and 8 women; 47 ± 12 yr) and 10 healthy subjects (5 men and 5 women; 43 ± 7 yr). The diagnosis of

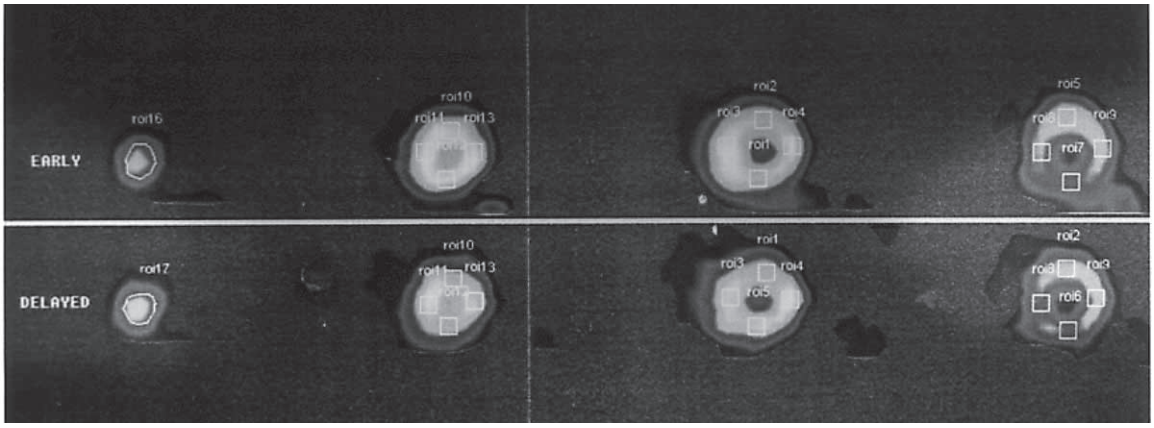

Fig. 1 Early and delayed short-axis SPECT images with regions of interest.

hypertrophic cardiomyopathy (HCM) was made when the patient had echocardiographic evidence of asymmetric septal hypertrophy (septal/free wall thickness > 1.5/1.0), a dynamic left ventricle outflow tract (LVOT) gradient and no apparent cause for the hypertrophy such as aortic valvular stenosis or systemic hypertension.[14] The frequencies of dyspnea, angina pectoris and syncope were recorded as symptoms and heart failure was classified according to the New York Heart Association (NYHA) classification.[15] The control group consisted of healthy subjects who had no significant stenosis on coronary angiography. The physical findings of the controls were normal. In addition, patients with underlying disease possibly causing left ventricular hypertrophy were excluded from this study.

Table 1 Echocardiographic results of each group

	Normal	ASH	p value
IVS (cm)	0.81 ± 0.28	2.14 ± 0.25	0.001
PW (cm)	0.88 ± 0.17	1.16 ± 0.22	0.002
LVEDD (cm)	4.85 ± 0.37	4.12 ± 0.44	0.001
LVESD (cm)	2.88 ± 0.48	2.55 ± 0.37	0.06
FS (%)	47.80 ± 11.91	41.22 ± 8.63	0.1
EF (%)	68.66 ± 9.91	68.25 ± 7.76	0.9

Values are expressed as mean ± SD. IVS = Interventricular septal thickness, PW = Posterior wall thickness of left ventricle, LVEDD = End-diastolic dimension of left ventricle, LVESD = End-systolic dimension of left ventricle, FS = Fractional shortening, EF = Ejection fraction.

Echocardiography

Two-dimensional and Doppler echocardiographic examinations were performed with an Acuson Sequoia C 256 machine (Acuson Corporation, Mountain View, CA, USA) with a 3.5 MHz transducer. Echocardiographic images were obtained from the parasternal long axis, short-axis, 4- and 2-apical chamber views with the patient supine in the left lateral decubitis position. M-Mode measurements were performed according to the criteria of the American Society of Echocardiography.[16]

Tetrofosmin Imaging Protocol

Following an overnight fast, intravenous injection of 1,110 MBq (30 mCi) Tc-99m tetrofosmin was performed at rest. Each subject was asked to drink a glass of milk 45 minutes after the injection to accelerate hepatobiliary clearance. Tomographic images of each subject were obtained 1 hour later (early images) and again 4 hours later (delayed images). Tomography was acquired using a rotating large field of view gamma camera (Starcam 4000i XR/T, GE) equipped with a low energy, all purpose parallel hole collimator and connected to a dedicated computer system. A 15% window centered at 140 keV provided energy discrimination. Images were obtained with 64 projections (25 sec/projection) over a semicircular 180 arch, which extended from the 45° right anterior oblique to the left posterior oblique position. The data were stored on a 64 × 64 matrix. Data processing was performed on a nuclear medicine computer system (Entegra, GE). After pre-processing with a Butterworth filter, a series of contiguous transaxial images of one pixel thickness (8.64 mm) were reconstructed using a filtered back-projection algorithm without attenuation and scatter correction. Using transaxial images, the short axis, vertical long axis and horizontal long axis of the left ventricle were re-oriented. The spatial resolution (FWHM) of the system was 3.8 mm. For quantitative measurement of tetrofosmin washout in the left ventricle, short-axis SPECT images were divided into 5 segments (anterior, septal, lateral, inferior wall and apex) at the base, middle and apex in early and delayed images. The mean radioactivity counts were measured in each segment by drawing regions of interest (ROIs) on the corresponding segments of 4 short-axis images for both early and delayed scans (Fig. 1). In the anterior, septal, lateral and inferior wall, box ROIs sized 9 × 9 pixels and in the apex, irregular ROI were used. ROIs drawn on early images were then mirrored on

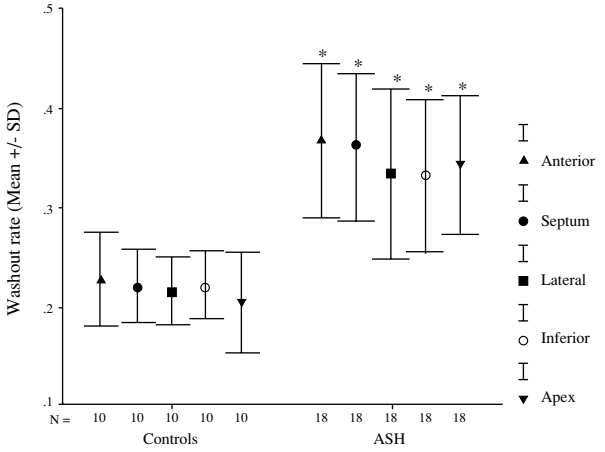

Fig. 2 Comparison of washout rates at each segment of each group. * $p < 0.001$ between control and ASH groups

the delayed images. The mean radioactivity counts of each segment in 4 short-axis images were averaged to yield a single segmental value. Washout rate of Tc-99m tetrofosmin was calculated for each segment using the following formula: washout rate = (mean counts for the initial image – mean counts of the delayed images)/mean counts of the initial images.

Statistical Analysis

Data are presented as mean ± standard deviation. SPSS PC for Windows version 10.0 was used for statistical analysis. The data were checked for normal distribution. Since the data were normally distributed, Student's t-test was used between groups. The relationship between washout rates and echocardiographic findings was evaluated by Pearson correlation test. A p value less than 0.05 was considered statistically significant.

RESULTS

The echocardiographic results of the patients with ASH and the control group are summarized in Table 1. In ASH, the washout rates at all myocardial segments were significantly increased compared to those of the normal controls. Washout rates of apex, anterior, septal, lateral and inferior walls were 0.34 ± 0.06, 0.37 ± 0.07, 0.36 ± 0.07, 0.33 ± 0.08, 0.33 ± 0.07 in ASH and 0.20 ± 0.05, 0.23 ± 0.05, 0.22 ± 0.03, 0.21 ± 0.03, 0.22 ± 0.03 in the normal group, respectively ($p < 0.05$) (Fig. 2).

Eight of 18 patients were asymptomatic. Seven patients suffered dyspnea and angina pectoris, whereas only two patients had history of syncope. According to the NYHA classification, 11 patients were in NYHA class I and 7 patients were in NYHA class II–III. The degree of Tc-99m tetrofosmin washout of all segments was significantly increased in patients with NYHA II–III compared to patients with NYHA I ($p < 0.05$) (Table 2). The correlation of washout and echocardiographic results is shown in Table 3. There was a significant positive correlation between the tetrofosmin washout and wall thicknesses of interventricular septal and posterior walls. The mean FS (%) and EF (%) were also found to be lower in ASH patients than the mean normal value, but the difference was not statistically significant (Table 1), and there were no statistically significant correlation between tetrofosmin washout and FS (%) – EF (%) (Table 3).

Table 2 Comparison of washout rates at each segment in patients with NYHA I and II–III

	NYHA I (n = 11)	NYHA II–III (n = 7)	p
Septal	0.32 ± 0.05	0.42 ± 0.05	0.001
Anterior	0.32 ± 0.05	0.44 ± 0.05	0.001
Lateral	0.29 ± 0.6	0.39 ± 0.08	0.02
Inferior	0.30 ± 0.07	0.38 ± 0.06	0.02
Apex	0.30 ± 0.04	0.40 ± 0.06	0.001

Table 3 Correlation between tetrofosmin washout and echocardiographic results

	Correlation coefficient					
	IVS	PW	SVEDD	SVESD	FS	EF
Anterior	0.72*	0.46**	–0.29	–0.11	–0.35	–0.04
Septal	0.74*	0.56*	–0.32	–0.21	–0.21	0.05
Lateral	0.64*	0.54*	–0.26	–0.13	–0.29	–0.06
Inferior	0.61*	0.50*	–0.27	–0.17	–0.23	0.03
Apex	0.73*	0.49*	–0.23	–0.01	–0.32	–0.13

* Correlation is significant at the 0.01 level (2-tailed).
** Correlation is significant at the 0.05 level (2-tailed).

DISCUSSION

Tc-99m tetrofosmin is a lipophilic, cationic diphosphine which has been developed for myocardial perfusion imaging.[17,19] Tc-99m tetrofosmin rapidly enters the myocardial cells related to myocardial perfusion and metabolism.[11,17,18] Mechanisms of Tc-99m tetrofosmin myocardial uptake have been studied by some authors using different experimental models. According to some of these studies mitochondrial membrane potential appears to play a major role in the myocardial uptake and retention of Tc-99m tetrofosmin. Platts et al.[20] studied the mechanism of Tc-99m tetrofosmin uptake in isolated adult rat heart. They found that Tc-99m tetrofosmin uptake by myocytes occurs via metabolism-dependent process that is not affected by cation channel inhibitors. Younes et al.[21] studied the mechanism of Tc-99m tetrofosmin uptake into isolated rat heart mitochondria and reported that the most likely mechanism for this is mediated by potential-driven diffusion of the lipophilic cation across the sarcolemmal and mitochondrial membranes. Arbab et al.[11] investigated the kinetics, cellular

uptake and intracellular distribution of Tc-99m tetrofosmin in tumor cell lines and concluded that Tc-99m tetrofosmin uptake depends on both cell membrane and mitochondrial potentials. Few studies are available on washout rates of Tc-99m tetrofosmin. Takahashi et al.[22] and Hirata et al.[23] reported increased washout rates in injured areas compared to normal areas. In Hirata et al's study increased washout rates of Tc-99m tetrofosmin in patients with acute myocardial infarction tended to disappear after successful reperfusion therapy 1–6 months later. They concluded that accumulated tracer might be released due to sarcolemmal and/or mitochondrial dysfunction caused by ischemia. The findings of the present study suggest that the Tc-99m tetrofosmin washout in patients with ASH was significantly higher than in the control group and the degree of tetrofosmin washout corresponded well with the severity of myocardial thickness of the interventricular septum and posterior walls. Our study also revealed that tetrofosmin washout was faster in patients with NYHA II–III compared to patients with NYHA I, suggesting that cardiac function is related to mitochondrial and/or sarcolemmal function. The pathophysiology of HCM is unclear. It has been shown in pathologic studies that myocyte disarray and abnormal myocytes are the most prominent microscopic features of HCM.[24–29] Within cells there is variation in nuclear size and disruption of myofibrillar architecture. The abnormal myocytes are often associated with areas of myocardial fibrosis, which are usually extensive involving the entire region of the left ventricular wall regardless of the presence or absence of hypertrophy.[30–34] So far, to our knowledge, there have been no pathologic studies on the functions of sarcolemma and/or mitochondria in HCM. In addition, in the literature there is only one scintigraphic study about the washout rates of Tc-99m tetrofosmin in HCM. In that study Morishita et al.[35] found increased myocardial washout rates of Tc-99m tetrofosmin in ASH patients like in our study.

CONCLUSION

The retention of Tc-99m tetrofosmin in the myocardium depends on the potentials of the cellular and mitochondrial membranes. In this study, increased myocardial washout retes of Tc-99m tetrofosmin in ASH patients were obtained not only at the hypertrophied region but also at nonhypertrophied regions consistent with pathologic studies. Also our study revealed that Tc-99m tetrofosmin washout was higher in NYHA II–III patients compared to NYHA I patients and the degree of Tc-99m tetrofosmin washout corresponded well with the thickness of the interventricular septum and posterior walls. Thus, the evaluation of mitochondrial and/or sarcolemmal abnormalities, based on the presence or absence of abnormalities in the washout rate of Tc-99m tetrofosmin showed that there could be dysfunction of sarcolemma and/or mitochondria in the entire left ventricle which would be important in the pathophysiology of this disease. Further pathophysiologic studies examining the dysfunction of mitochondria and sarcolemma in this disease and patient follow-up data are needed in a prospective study to determine the prognostic value of Tc-99m tetrofosmin washout imaging in ASH patients.

REFERENCES

1. Report of the 1995 World Health Organization/International Society and Federation of Cardiology task force on the definition and classification of Cardiomyopathies. *Circulation* 1996; 93: 841–842.
2. Goodwin JF. The frontiers of cardiomyopathy. *Br Heart J* 1982; 48: 1.
3. Henry WL, Clark CE, Epstein SE. Asymmetric septal hypertrophy (ASH): echocardiographic identification of the pathognomonic anatomic abnormality of IHSS. *Circulation* 1973; 47: 225–233.
4. Goodwin JF. Prospects and predictions for the cardiomyopathies. *Circulation* 1974; 50: 210–219.
5. Marian AJ. Pathogenesis of diverse clinical and pathological phenotypes in hypertrophic cardiomyopathy. *Lancet* 2000; 355: 58–61.
6. Elliott PM, McKenna WJ. Hypertrophic cardiomyopathy. In: *Cardiology*, Crawford MH, DiMarco JP (eds), London; Mosby, 2001: 12.1–12.12.
7. Van Noorden S, Olsen EG, Pearse AG. Hypertrophic obstructive cardiomyopathy: A histological, histochemical and ultrastructural study of biopsy material. *Cardiovasc Res* 1971; 5: 118–131.
8. Maron BJ, Sato N, Roberts WC, Edwards JE, Chandra RS. Quantitative analysis of cardiac muscle cell disorganisation in the ventricular septum: comparison of fetuses and infants with and without congenital heart disease and patients with hypertrophic cardiomyopathy. *Circulation* 1979; 60: 685–696.
9. Sridhara BS, Braat S, Rigo P, Itti R, Cload P, Lahiri A. Comparison of myocardial perfusion imaging with technetium-99m tetrofosmin versus thallium-201 in coronary artery disease. *Am J Cardiol* 1993; 72: 1015–1019.
10. Jain D, Wackers FJ, Mattera J, McMahon M, Sinusas AJ, Zaret BL. Biokinetics of Technetium-99m-tetrofosmin: myocardial perfusion imaging agent: implications for a one-day imaging protocol. *J Nucl Med* 1993; 34: 1254–1259.
11. Arbab AS, Koizumi K, Toyama K, Araki T. Uptake of Technetium-99m-Tetrofosmin, Technetium-99m-MIBI and Thallium-201 in Tumor Cell Lines. *J Nucl Med* 1996; 37: 1551–1556.
12. Arbab AS, Koizumi K, Toyama K, Arai T, Araki T. Technetium-99m-Tetrofosmin, Technetium-99m-MIBI and Thallium-201 Uptake in Rat Myocardial Cells. *J Nucl Med* 1998; 39: 266–271.
13. Pauwels EK, McCready VR, Stoot JH, van Deurzen DF. The mechanism of accumulation of tumour-localising radiopharmaceuticals. *Eur J Nucl Med* 1998; 25: 277–305.
14. Maron BJ, Bonow RO, Cannon RO 3rd, Leon MB, Epstein SE. Hypertrophic cardiomyopathy: interrelations of clinical manifestations, pathophysiology and therapy. *N Engl J*

Med 1987; 316: 844–852.
15. The criteria committee of the New York Heart Association. *Nomenclature and criteria for diagnosis*. 9th ed., Boston; Little Brown, 1994.
16. Sahn DJ, DeMaria A, Kisslo J, Weyman A. Recommendations regarding quantitation in M-Mode echocardiography: result of a survey of echocardiographic measurements. *Circulation* 1978; 58: 1072–1083.
17. Gerson MC. New investigational Tc-99m compounds. In: *Cardiac SPECT imaging*, DePuey EG, Berman DS, Garcia EV (eds), Philadelphia; Lippincott-Raven, 1996: 157–167.
18. Kelly JD, Forster AM, Higley B, Archer CM, Booker FS, Canning LR. Technetium-99m-tetrofosmin as a new radiopharmaceutical for myocardial perfusion imaging. *J Nucl Med* 1993; 34: 222–227.
19. Rigo P, Leclercq B, Itti R, Lahiri A, Braat S. Technetium-99m-tetrofosmin myocardial imaging: a comparison with thallium-201 and angiography. *J Nucl Med* 1994; 35: 587–593.
20. Platts EA, North TL, Pickett RD, Kelly JD, Mechanism of uptake of technetium-tetrofosmin. I: Uptake into isolated adult rat ventricular myocytes and subcellular localization. *J Nucl Cardiol* 1995; 2: 317–326.
21. Younes A, Songadele JA, Maublant J, Platt R, Veyre A. Mechanism of uptake of technetium-tetrofosmin. II: Uptake into isolated adult rat heart mitochondria. *J Nucl Cardiol* 1995; 2: 327–333.
22. Takahashi N, Dahlberg ST, Gilmore MP, Leppo JA. Effects of acute ischemia and reperfusion on the myocardial kinetics of technetium 99m-labeled tetrofosmin and thallium-201. *J Nucl Cardiol* 1997; 4: 524–531.
23. Hirata Y, Takamiya M, Kinoshita N, Yamada H, Shima T, Miyazaki H. Interpretation of reverse redistribution of Tc-99m-tetrofosmin in patients with acute myocardial infarction. *Eur J Nucl Med* 2002; 29: 1594–1599.
24. Maron BJ, Wolfson JK, Roberts WC. Relation between extent of cardiac muscle cell disorganization and left ventricular wall thickness in hypertrophic cardiomyopathy. *Am J Cardiol* 1992; 70: 785–790.
25. Maron BJ, Roberts WC. Hypertrophic cardiomyopathy and cardiac muscle cell disorganization revisited: relation between the two and significance. *Am Heart J* 1981; 102: 95–110.
26. Maron BJ, Anan TJ, Roberts WC. Quantitative analysis of the distribution of cardiac muscle cell disorganization in the left ventricular wall of patients with hypertrophic cardiomyopathy. *Circulation* 1981; 63: 882–894.
27. Maron BJ, Sato N, Roberts WC, Edwards JE, Chandra RS. Quantitative analysis of cardiac muscle cell disorganization in the ventricular septum: comparison of fetuses and infants with and without congenital heart disease and patients with hypertrophic cardiomyopathy. *Circulation* 1979; 60: 685–696.
28. Maron BJ, Roberts WC. Quantitative analysis of cardiac muscle cell disorganization in the ventricular septum of patients with hypertrophic cardiomyopathy. *Circulation* 1979; 59: 689–706.
29. Maron BJ, Epstein SE. Hypertrophic cardiomyopathy. Recent observations regarding the specificity of three hallmarks of the disease: asymmetric septal hypertrophy, septal disorganization, and systolic anterior motion of the anterior mitral leaflet. *Am J Cardiol* 1980; 45: 141–154.
30. Maron BJ, Epstein SE, Roberts WC. Hypertrophic Cardiomyopathy and Transmural Myocardial Infarction without Significant Atherosclerosis of the Extramural Coronary Arteries. *Am J Cardiol* 1979; 43: 1086–1102.
31. Maron BJ, Wolfson JK, Epstein SE, Roberts WC. Intramural (“small vessel”) coronary artery disease in hypertrophic cardiomyopathy. *J Am Coll Cardiol* 1986; 8: 545–557.
32. Roberts WC, Ferrans VJ. Pathologic anatomy of the cardiomyopathies. Idiopathic dilated and hypertrophic types, infiltrative types and endomyocardial disease with and without eosinophilia. *Hum Pathol* 1975; 6: 287–342.
33. Tanaka M, Fujiwara H, Onodera T, Wu DJ, Hamashima Y, Kawai C. Quantitative analysis of myocardial fibrosis in normals, hypertensive hearts, and hypertrophic cardiomyopathy. *Br Heart J* 1986; 55: 575–581.
34. Waller BF, Maron BJ, Epstein SE, Roberts WC. Transmural Myocardial Infarction in Hypertrophic Cardiomyopathy: a cause of conversion from left ventricular asymmetry to symmetry and from normal-sized to dilated left ventricular cavity. *Chest* 1981; 79: 461–465.
35. Morishita S, Kondo Y, Nomura M, Miyajima H, Nada T, Ito S. Impaired Retention of Technetium-99m Tetrofosmin in Hypertrophic Cardiomyopathy. *Am J Cardiol* 2001; 87: 743–747.